Zirconia implants with improved attachment to the gingival tissue

Khalil Shahramian[*,†], Michael Gasik[‡], Ilkka Kangasniemi[†], Frank Walboomers[§], Jaana Willberg [,¶], Aous Abdulmajeed[#], Timo Närhi[*,†,]**

[*]Department of Prosthetic Dentistry and Stomatognathic Physiology, Institute of Dentistry, University of Turku, FI-20520 Turku, Finland

[†]Turku Clinical Biomaterials Center (TCBC), University of Turku, 20520 Turku, Finland

[‡]School of Chemical Engineering, Aalto University Foundation, FI-00076 AALTO, Espoo, Finland

[§]Biomaterials, Radboud University Nijmegen Medical Center, Nijmegen, Netherlands

Department of Oral Pathology and Radiology, Institute of Dentistry, University of Turku, FI-20520 Turku, Finland

[¶]Department of Pathology, Turku University Central Hospital, FI-20520 Turku, Finland

[#]Department of General Practice, School of Dentistry, Virginia Commonwealth University, Richmond, Virginia

[**]City of Turku, Welfare Division, Oral Health Care, Turku, Finland, FI-20520 Turku, Finland

All authors meet the ICMJE for authorship and have agreed to the submission of the work presented here to *Journal of Periodontology*.

Summary Sentence: The gingival tissue is more strongly attached to sol-gel derived TiO2 coated zirconia than uncoated zirconia.

Running title: Gingival tissue attachment to zirconia.

This is the author manuscript accepted for publication and has undergone full peer review but has not been through the copyediting, typesetting, pagination and proofreading process, which may lead to differences between this version and the Version of Record. Please cite this article as doi: 10.1002/JPER.19-0323.

Correspondence to: Khalil Shahramian

Department of Prosthetic Dentistry and Stomatognathic Physiology, Institute of Dentistry, University of Turku, Lemminkäisenkatu 2, FI-20520 Turku, Finland

Fax: +358 (0)2 333 8390

Tel: +358 (0) 2 333 8530

E-mail:khalsha@utu.fi

Abstract

Background: Gingival tissue attachment is known to be important for long term prognosis of implants. This in vitro study evaluated the gingival attachment to zirconia implants and zirconia implants modified with sol-gel derived TiO_2 coatings.

Materials and methods: Zirconia endodontic posts (n=23) were used to function as implants that were inserted into the center of full thickness porcine gingival explants (n=31). The tissue/implant specimens were then individually placed at an air/liquid interface on a stainless-steel grid in cell culture wells containing a nutrient solution. The tissue cultures were incubated at 37ºC in a 5 % CO_2 environment and at days 7 and 14, the specimens were harvested and analyzed by dynamic mechanical analysis (DMA) measurements under dynamic loading conditions mimicking natural mastication. Specimens were also analyzed by immunohistochemical staining identifying the laminin (Ln) γ2 chain specific for Ln-332, which is known to be a crucial molecule for the proper attachment of epithelium to tooth/implant surface.

Results: Tissue attachment to TiO_2 coated zirconia demonstrated higher dynamic modulus of elasticity and higher creep modulus, meaning that the attachment is stronger and more resistant to damage during function over time. Laminin γ2 was identified in the attachment of epithelium to TiO_2 coated zirconia.

Conclusion: Both DMA and histological analysis support each other, that the gingival tissue is more strongly attached to sol-gel derived TiO_2 coated zirconia than uncoated zirconia. Immunohistochemical staining showed that TiO_2 coating may enhance the synthesis and deposition of Ln-332 in the epithelial attachment to the implant surface.

Keywords:

Dental materials, Implantology, Biomaterial(s), Prosthodontics, Periodontitis

.

1. Introduction

Success of a dental implant depends on a sound osseointegration and a stable attachment to the surrounding tissue.[1–3] The establishment of a healthy permucosal seal protects the underlying tissues from the harsh intraoral environments.[1–3] The ability of an implant abutment to form a firm bond with its surrounding gingival tissue is highly dependent on its biocompatibility, surface topography, and surface free energy.[2,4] These properties are key influencing factors in adhesion, proliferation and colonization of cells involved in the wound healing process around the abutment and the subsequent attachment to the surrounding tissue.[2] Despite the plenty of research conducted on the interface of implants and bone, till date, our knowledge of soft-tissue/implant interface is limited [5] and further research evaluating the interface with different implant materials is necessary. Furthermore, developing new implant materials or optimizing current materials to truly bond with surrounding soft-tissue is important. The structure responsible for the attachment of soft-tissue to implants is the peri-implant epithelium (PIE) and several studies have shown that this attachment occurs in the presence of several attachment structures.[6–9] An important component of the basal lamina that attaches the PIE and the junctional epithelium (JE) to implants and teeth respectively, is laminin (Ln)-332.[6,10] Laminins are glycoproteins that are an integral part of the structure of basement membranes that attach epithelial cells to the connective tissue.[6,10,11] For example, Ln-332 is a major component involved in this process and *in vitro* studies have shown that it is critical for gingival epithelial cell attachment.[11–13] Also, Ln-332 is secreted by keratinocytes after an injury to initiate migration of epithelial cells and to repair the basement membrane and re-create the anchorage of epithelial cells to the basement membrane.[14–16] Therefore, the presence of Ln-332 at soft-tissue/implant interface identifies an established attachment and a bond between epithelial cells and the biomaterial. Furthermore, Ln-332 is composed of three chains, $\alpha 3$, $\beta 3$, and $\gamma 2$.[11] Antibodies targeting the $\gamma 2$ chain are specific for Ln-332. Most research on soft-tissue/implant interface have focused on titanium substrates, while implant dentistry is facing a rapid introduction

of alternative materials with different surface optimizations. An increasingly used material is zirconia that is claimed to have superior biological, esthetic, and optical properties.[1,2,17–20] Research evaluating soft-tissue/zirconia interface is still limited and data on surface optimizations of zirconia are scarce. Sol-gel derived TiO_2 surface treatments are one example of implant surface optimization that can be applied on zirconia to improve the soft tissue attachment. The potentials of these coatings to optimize zirconia for better soft-tissue attachment have been previously demonstrated by the authors where the coatings enhanced fibroblast proliferation and induced a faster blood coagulation.[21,22] Furthermore, *in vivo* studies with experimental animals utilizing sol-gel derived TiO_2 coatings on titanium substrates have shown good epithelial attachment, decreased gingival inflammation and less marginal bone loss upon histological examination.[21–26]

Consequently, the aim of this study was to evaluate the attachment of gingival tissue on zirconia implant and zirconia provided with sol-gel derived nanostructured coating. This was done in conjunction with a non-destructive mechanical bonding analysis. The aim was set based on the lack of research on both soft-tissue/zirconia interface, and the lack of efforts towards optimization of zirconia for better biological properties. It was hypothesized that sol-gel derived coatings enhance the attachment. Furthermore, the interface between the materials and the soft-tissue was analyzed using special dynamic mechanical analysis (DMA) to evaluate the quality of the attachment apparatus in both groups. The present study is a part of a series of studies attempting to improve the biological properties of zirconia implant abutments.

2. Materials and Method

2.1. Implant preparation

Zirconia endodontic posts* obtained from a local supplier were used to function as implants that were inserted in porcine gingival tissue, mimicking the clinical attachment of abutments to soft-tissue intraorally. Each endodontic post was cut in half using a surgical saw to yield implantable materials with length of 9 mm and diameters of 1.90±0.02 mm (n=23). The implants were then cleaned in ultrasonic baths of acetone and ethanol subsequently for 5 min each. Two experimental groups were made, zirconia coated with sol-gel derived TiO_2, and uncoated zirconia as control. The sol-gel solution was made by dissolving tetraisopropylorthotitanate [$Ti(OCH(CH_3)_2)_4$] in 95% ethanol and mixing it with a solution of ethanol, nitric acid and ultrapure water. The resultant solution was left to age at room temperature for 24 h. The TiO_2 coatings were prepared by dipping the specimens into the solution and then withdrawing them at a speed of 0.3mm/s. Finally, the coated specimens were heated at 500°C for 1 h and were again cleaned ultrasonically as described before.

2.2. Implantation and tissue culture

For immunohistochemical studies, full thickness gingival explants were dissected from mandible of a freshly slaughtered pig using a 6 mm biopsy punch (n=19) and then rinsed in PBS supplemented with penicillin, streptomycin and amphotericin B. The explants were pierced using an 18-gauge needle to mimic the surgical wound created clinically during implant placement. Each of the implants was autoclaved for 20 min at 121ºC and then inserted into the center of the explants so that the implant penetrated the gingival explant. A total of 15 tissue/implant specimens were then individually placed at an air/liquid interface on a stainless steel grid, in 6-well plates containing culture medium† supplemented with 10 % fetal bovine serum (FBS), 100 U/lg penicillin, streptomycin 100 lg/m L, and

200 mM L-glutamine (Figure 1). The specimens were incubated at 37ºC in a 5 % CO_2 environment with the culture medium changed every 24 hours up to 7 (4 samples with a non-coated implant, 4 samples with a coated implant) and 14 days (3 samples with a non-coated implant, 4 samples with a coated implant) in culture. At the end of each tissue culture period, the specimens were fixed in 10% buffered formalin for 1 day at room temperature, after which they were sent for immunohistochemical analysis. Gingival explants with no implants were also cultured to serve as baseline controls for general tissue morphology (n=2/time-point).

For DMA measurements, a total of 8 tissue/implant specimens were obtained from the mandible of a second pig and they were cultured according the same protocol at the same time points (n=2 for coated and normal specimens/time-point). Gingival explants with no implants were also cultured to serve as baseline controls (n=2/time-point).

2.3. Biomechanical measurement with DMA

The dynamic modulus and creeping modulus of the interface between the gingival tissue and the implants in shear mode were measured using a novel protocol[‡] in a dynamic mechanical analyzer[§]. The specimens (i.e. gingival explants attached to the implants) were placed on the specimen holder of the analyser (n=2 for coated and uncoated implants in both time points). The setup applies oscillating sinusoidal force to the implants as shown in Figure 2, straining them and creating displacement amplitude of 30µm. The forces were applied at a constant frequency of 1 Hz at 37°C, mimicking the cyclic masticatory rhythm and human body temperature.[27] For this specific setup and geometry, the geometric factor k_2 was experimentally determined as:[28]

$$k_2 = 0.7386\left(1-\left(\frac{r_a}{r_2}\right)^3\right)$$

where r_2 is the radius of the specimen holder, r_a is the radius of the implant.[28]

Thus, the dynamic elastic modulus can be expressed as:[28]

$$E_{dyn} = k_2 \frac{F_{dyn}\, r_2^2}{(h_0 + dL)^3 |A_s|}$$

and the tangential (creeping) elastic modulus as:[28]

$$E_{stat} = k_2 \frac{F_{stat}\, r_2^2}{(h_0)^3 |dL|}$$

where F_{dyn} is the dynamic force amplitude on the specimen, F_{stat} is the static acting force, h_0 is the initial height of the tissue, dL is the change of the height during the measurement, and A_s is the displacement amplitude of a specimen.[28] The dimensions of each specimen were measured using a laser micrometer prior to their placement in the analyzer with a tolerance of ±1 µm.

For assessment of realistic stresses and displacements a 2D-axyisymmetric model was set up using a software to estimate the distribution of the deformation inside the soft tissue attached to the implant, assuming the latter to be a rigid solid. This model was served as a visual guidance as exact properties of the soft tissue are not known in these conditions. Figure 2 (right) shows maximal total displacements (color scale), surface traction forces (vector arrows) and von Mises stresses (contours) indicating that most of the traction forces are indeed localized at the tissue/implant interface.

2.3.1. Embedding of tissue culture samples

A modification of the previously shown embedding method using a novel polymerization system¶ was used.[29,30] The polymerization system¶ is based on polymethyl metacrylate (PMMA). Polymerization occurs in the absence of oxygen and at low temperatures (-2 to -20°C) and enables to perform immunohistochemical staining for hard tissues.[29] It is especially suitable for the studies of implant-tissue interface.[29] The embedding procedure involves four major steps; (i) fixation and dehydration, (ii) pre-infiltration, (iii) infiltration, and (iv) polymerization. Each of these steps require the use of different solutions that were prepared by mixing different chemicals in different ratios as summarized in Figure 3, a modification of the manufacturer's protocol.

After fixation, the specimens were washed for several hours with running tap water, and then dehydrated by placing them overnight in a series of alcohol and xylene at room temperature in the following steps; 70% alcohol, 96% alcohol, twice 100% alcohol, twice xylene. Following dehydration, the specimens were placed overnight in pre-infiltration solution 1 and then overnight in pre-infiltration solution 2, both at room temperature. Consequently, the samples were placed in pre-infiltration solution 3 and then in the infiltration solution, while incubated at +4°C overnight during both steps.

For polymerization of the tissue, 45 mL of stock A solution and 5 mL of stock B solution were carefully mixed. Each tissue sample was placed on the bottom of a precooled Teflon mold stored at +°4C with plastic forceps and the polymerization solution was added into the mold. Then, the tissue samples were placed into a vacuum desiccator cooled down to -4°C. The samples were evacuated in

-4°C in 200-400mbar around 30 min or as long as any gas bubbles were detected. The pressure was let out of the vacuum desiccator and the molds were closed with their covers. The desiccator was closed and stored in -4°C for polymerization for 2 days. The hardened tissue blocks were pulled out of the molds.

2.3.2. Sectioning

The tissue blocks were first glued on plastic slides using a photocuring adhesive[#]. The surfaces of the blocks were ground using K400 and polished with K1000 diamond discs[**]. A second glass slide was roughened using a silicon carbide P500 paper[**]. The glass slide was washed in distilled water and the surface was cleaned with 100% alcohol and then one drop of primer[††] was put in the middle of the glass slide and the slide was let to dry for 1 minute. A drop of adhesive[#] was placed on top of the tissue block and the glass slide was glued onto the tissue block-plastic slide complex using a gluing machine[**] utilizing UV light for 15 minutes. The tissue block was hence sandwiched between two slides. Sample sandwich was clamped onto a diamond band saw[**] and 100µm thick sections were cut. After that, the sections were ground using K400, K1000 diamond discs[**] and then P1200, P2500 and P4000 silicon carbide papers[**] until the thickness of 20 µm was achieved.

2.3.3. Immunohistological analysis

Before immunohistochemical staining, deplastination of the methyl methacrylate-embedded sections was performed. The slides were incubated twice in xylene, twice in methoxy methyl acetate, twice in acetone and twice in distilled water. The sections were then rinsed by Phosphate Buffer Saline (PBS) and incubated in 0.05% trypsin for 15 minutes at room temperature. Sections were washed again in PBS, (3 times, 5 min each). This washing procedure was repeated between each step. After the wash in PBS, the sections were incubated at room temperature in a bath of 3%

hydrogen peroxide for 30 minutes. Moving on, the PBS wash was repeated, and the sections were incubated at room temperature in 10% bovine serum albumin for 30 minutes. The sections were washed again with PBS and incubated overnight at 4°C in a 1:100 dilution of goat polyclonal IgG laminin γ2 antibody. [‡‡]

PBS wash was repeated, and the sections were incubated at room temperature in a dilution of secondary antibody anti-goat[§§] (3 anti-goat:4 diluent) for 30 minutes, washed again in PBS and finally with diaminobenzidine (DAB). After the wash in PBS, the sections were counterstained by placing them in hematoxylin for 1 minute at room temperature, dried, and covered with a rapid drying medium . All sections were analyzed under a light microscope[¶¶] and the images were captured using a digital camera[##] and an imaging software. [***]

3. Results

Figures 4A and 4B display the mean values and standard deviations of the calculated dynamic elastic moduli and creep moduli, respectively. Coated zirconia implants showed substantially higher dynamic modulus compared to uncoated control at both days 7 (+88% vs. control) and 14 (+109%) (Figure 4A). Similarly, under creeping conditions (pseudo-static) the modulus of adhesion was also higher for the coated specimens at both days 7 (+5%) and 14 (+55%) (Figure 4B). Figure 5 shows how the differences were calculated.

As a positive control, laminin γ2 chain appeared as an immunoreactive band in the basement membrane zone of the porcine gingival tissue cultured in vitro (Figure 6A). The epithelial cells of the gingival explants were seen to have migrated in order to cover the exposed connective tissue, proving that the explants were vital throughout the culture period (data not shown). In the sections

harvested at the 7 days of culture, both epithelial and connective tissue were firmly attached to the implant surface (Figures 6B, 6C, 6D). Laminin γ2 chain stained positively in the most apical cells of the epithelium in contact with the coated implant surface and also in the basement membrane facing the connective tissue (Figure 6C).

There was no staining of laminin γ2 detected at the contact of epithelium with non-coated zirconia at day 7 (Figure 6D). Sections from day 14 of culture also revealed a firm attachment of epithelium and connective tissue to the coated implant surfaces (Figures 6E, 6G, 6H). Laminin γ2 was present in the innermost cells of the apical two thirds of the epithelium attached to the implant (Figures 6E, 6G). Although sloughing of gingival epithelial cells appeared (a phenomenon that happened in the epithelium of all tissue explants), the attachment of the epithelium to the coated implant seemed to be firm (Figure 6H). After 2 weeks culture with non-coated implants, the tissue detached from the implant surface during cutting the sections. There were a few spots of faint positive staining of laminin γ2 detected at the epithelial cells that had been attached to the implant (Figure 6F). In both non-coated and coated zirconia implants, the epithelium did not show apical migration between the explant and the implant surface, which allows maturation of connective tissue attachment.

4. Discussion

The term "peri-implant mucosa" is given to the soft tissue collar that surrounds the transmucosal part of a dental implant and thereby separates the peri-implant bone from the oral cavity.[31] Attachment of the peri-implant mucosa to the implant creates a seal that potentially prevents the development of peri-implant mucositis and peri-implantitis, contributing to the long term survival of the implant.[31] This attachment is provided by the PIE, which is the implant-counterpart of the JE present with natural dentition. The peri-implant mucosa forms after the closure of the

mucoperiosteal flap in a one-stage or two-stage implant surgery through the healing of the wound created during the surgical placement of an implant.[31] The process of wound healing around implant starts immediately during the surgery by protein adsorption on implant or abutment surface, followed by the formation of a blood clot at the site of surgical wound. The wound is rapidly sealed off by the blood clot and later on, this fibrin clot induces an inflammatory process that leads to tissue formation and remodeling.[31–35] The potentials of sol-gel derived TiO_2 to enhance blood coagulation and hence hasten wound healing process have been previously demonstrated by the authors.[22] This study attempted to investigate the formation of the soft tissue attachment in contact with the coated zirconia and to test the strength of the attachment. Wong et al. 2009 demonstrated that porcine and human oral mucosal wounds are similar in terms of molecular composition and clinical and histological characteristics.[36] Hence, porcine gingival mucoperiosteal explants were used in this study. Furthermore, in order to resemble the wound and mucoperiosteal flap created during one-stage or two-stage implant surgery in human oral mucosa, the explants were pierced with a needle prior to the placement of the sample implants. In addition, Abdulmajeed et al. 2015 reported that this experimental setting has the advantages of being cost effective, time efficient, and easy to control the setup since delicate biological processes are not disrupted by animal movements.[37] The literature agrees that the peri-implant mucosa resembles scar tissue, having fewer fibroblasts and more collagen fibers when compared to tissue around teeth.[31,38] Moreover, because of a lack of the cementum layer with implants, the collagen fibers in the peri-implant mucosa are oriented parallel or parallel-oblique to the implant surface.[31,39] Reports on soft-tissue contact with zirconia are limited and although some reports state the presence of no difference between the tissue in contact with zirconia and titanium, others report a better biocompatibility of zirconia. [1,2]

Immunohistochemical analyses were utilized to identify the γ2 chain of Ln-332 as an indication of gingival epithelial attachment to uncoated and coated zirconia. An advanced embedding technique has been previously shown to be applicable for immunohistochemical studies with non-calcified teeth and implants.[40,41] The works of Atsuta et. al. have previously identified the presence of Ln-332 in the peri-implant epithelium in contact with titanium.[6,10] They reported the distribution of Ln-332 in the basal cells of the PIE already 3 days after implantation.[10] Two weeks after implantation Ln-332 was strongly expressed at the PIE-implant interface despite the upper portion of the epithelium. The results of this study and the distribution of Ln-332 in the PIE around zirconia coated with TiO_2 are in agreement with the works of Atsuta et. al.[6, 10] TiO_2 coating seems to enhance the synthesis and deposition of Ln-332 in the epithelial attachment to the implant surface. Also the connective tissue attachment to the implant surface is firm and tight. The results of the dynamic modulus analyses also support the histological findings. It may be inferred that tissue attachment to zirconia abutments is inferior to that of titanium and that zirconia abutments require further optimization to achieve soft-tissue attachment. This optimization was attempted in this study through sol-gel derived TiO_2 coatings.

It is unknown and difficult to estimate how much attachment is needed clinically in order to resist an inflammatory breakdown of the seal. However, this was attempted in another experiment by Atsuta et. al.[42] where horseradish peroxidase (HPR) test was used to mimic bacterial ingression into the gingiva surrounding zirconia and titanium. HPR was found in the connective tissue under the PIE around zirconia and it was concluded that zirconia implants had a weaker seal with epithelial tissue and were at higher risk of infection compared to titanium counterparts.

It is noteworthy that keeping the tissue explant alive and dynamic for a long culture period is obviously a challenge in this tissue culture model, and some changes seen in the histological images of 14 days cultures may partly be explained by beginning loss of tissue cohesion.[37] Moreover, preservation of both the morphology and immunogenity of the implant-soft tissue attachment is a challenge for the histological protocol. Hard and soft tissues would demand different modifications of histological working procedures. However, the presented method has its advantages compared to mechanical removal of the gingival tissue from the implant surface, when all cell adhesion molecules may not be preserved. Sawing and grinding the implant samples causes friction which may lead to artefacts like tissue rupturing and detachment of soft and hard tissues. In this study, it was concluded that detachment of gingival soft tissue from the uncoated implant surface was also due to less favorable cell adhesion compared to coated samples. With coated samples, the epithelial tissue seemed to be tightly attached to the implant surface although there were ruptures within the connective tissue. Better tissue morphology could possibly be achieved by grinding the sections by hand with diamond discs. In addition, cutting very thin sections of zirconia is not technically possible which may cause problems for immunohistochemical studies and microscopic examination of the sections.

Soft tissues, including the gingival tissue, and the attachment apparatus formed between them and a dental implant abutment, are viscoelastic in nature.[43–45] A viscoelastic material is a material that exhibits both elastic and viscous characteristics, i.e., its behavior contains both elastic and dissipative components of deformation.[46,47] Elastic materials deform under stress and return to their original state when the stress is removed, while viscous materials return over time to a state similar, but not identical, to the original state.[47] In addition, teeth, gingival tissue and dental materials including implants, are constantly subject to repetitive forces of mastication. For such materials, dynamic tests

such as dynamic mechanical analysis provide more relevant information about their properties than traditional static tests. During dynamic testing, a specimen undergoes a load of sinusoidal deformation (strain) at a frequency and the corresponding forces or deformations are measured.[48] With viscoelastic materials, the strain lags behind the stress, with the material undergoing deformation and reformation back to the original state simultaneously as the next round of cyclic loads are applied.[48] This study involved the application of oscillating forces in shear, similar to that of mastication at the physiological frequency (1 Hz), to the specimens and the response of the attachment apparatus to deformation was analyzed. Most research in the literature testing mechanical properties of dental materials and implants traditionally implement static methods of evaluation.[39,46,49] The information provided by these tests are associated with a longer time scale than that of mastication and can be a source of misleading results.[46] Dynamic methods are preferred and are more clinically relevant because they mimic the cyclic masticatory loading to which materials are subjected. The higher dynamic modulus reported with TiO_2 coated zirconia specimens, together with the immunohistochemical analyses, translates to a proof of stronger attachment with the surrounding tissue. Similarly, under pseudo-static (creeping) conditions, a higher force will be required to cause sliding of TiO_2 coated zirconia implants to the same arbitrary deformation when compared to uncoated implant/tissue complexes. Although the low sample number utilized in the study might be regarded as a limitation, the differences observed are the result of comparison of several data sets obtained from each sample and are substantial enough to draw conclusions. [50]

Conclusively, the clinical implication of this study is that the coated zirconia abutments have a stronger attachment to the surrounding gingiva and hence resist trauma and bacterial attack for a longer time. The coatings help in providing a separation of the intraoral and peri-implant environments, and their attachment to the surrounding soft tissue undergoes less deformation over

time when the implants are in function. Even with the presented limitations, this study indicates the benefits of the coated zirconia abutments and enables their application for more research in clinical environments to further understand their properties and the mechanism by which their bond forms with the surrounding gingiva.

5. Conclusion

This study shows the distribution of Ln γ2 chain in the developing epithelial attachment with zirconia. The early synthesis and deposition of Ln-332 in the epithelial bond with sol-gel derived TiO_2 coatings on zirconia may enhance soft tissue attachment. Under physiological dynamic loading, a stronger attachment was observed with TiO_2 coated zirconia compared with uncoated zirconia.

6. Acknowledgement

Authors are grateful to M.Sc. Heta Närhi (Aalto University Foundation, Finland) for carrying out DMA measurements and to Dr. Yevgen Bilotsky (Seqvera Ltd., Finland) for BEST data processing (US Pat. 10,379,106 B2) and analysis, Katja Läpikivi (Institute of Dentistry, University of Turku) and Mariia Valkama (Institute of Dentistry, University of Turku) for their technical assistance. Hammasväline Finland is gratefully acknowledged for donating the zirconia endodontic posts.

7. References

1. Linkevicius T, Vaitelis J. The effect of zirconia or titanium as abutment material on soft peri-implant tissues: A systematic review and meta-analysis. *Clin Oral Implants Res* 2015;26:139–47.

2. Van Brakel R, Meijer GJ, Verhoeven JW, Jansen J, De Putter C, Cune MS. Soft tissue response to zirconia and titanium implant abutments: An in vivo within-subject comparison. *J Clin Periodontol* 2012;39:995–1001.

3. An N, Rausch-Fan X, Wieland M, Matejka M, Andrukhov O, Schedle A. Initial attachment, subsequent cell proliferation/viability and gene expression of epithelial cells related to attachment and wound healing in response to different titanium surfaces. *Dent Mater* 2012;28:1207–14.

4. Wennerberg A, Sennerby L, Kultje C, Lekholm U. Some soft tissue characteristics at implant abutments with different surface topography. A study in humans. *J Clin Periodontol* 2003;30:88–94.

5. Rupp F, Liang L, Geis-Gerstorfer J, Scheideler L, Hüttig F. Surface characteristics of dental implants: A review. *Dent Mater* 2018;34:40–57.

6. Atsuta I, Yamaza T, Yoshinari M, et al. Ultrastructural localization of laminin-5 (γ2 chain) in the rat peri-implant oral mucosa around a titanium-dental implant by immuno-electron microscopy. *Biomaterials* 2005;26:6280–7.

7. McKinney R V., Steflik DE, Koth DL. Evidence for a junctional epithelial attachment to ceramic dental implants. *J Periodontol* 1985;56:579–91.

8. Gould TRL, Westbury L, Brunette DM. Ultrastructural study of the attachment of human gingiva to titanium in vivo. *J Prosthet Dent* 1984;52:418–20.

9. Donley TG, Gillette WB. Titanium endosseous implant-soft tissue interface: a literature review. *J Periodontol* 1991;62:153–60.

10. Atsuta I, Yamaza T, Yoshinari M, et al. Changes in the distribution of laminin-5 during peri-implant epithelium formation after immediate titanium implantation in rats. *Biomaterials* 2005;26:1751–60.

11. Walko G, Castañón MJ, Wiche G. Molecular architecture and function of the hemidesmosome. *Cell Tissue Res* 2015;360:529–44.

12. El-Ghannam A, Starr L, Jones J. Laminin-5 coating enhances epithelial cell attachment, spreading, and hemidesmosome assembly on Ti-6A1-4V implant material in vitro. *J Biomed Mater Res* 1998;41:30–40.

13. Tamura RN, Oda D, Quaranta V, et al. Coating of titanium alloy with soluble laminin-5 promotes cell attachment and hemidesmosome assembly in gingival epithelial cells: potential application to dental implants. *J Periodontal Res* 1997;32:287–94.

14. Kainulainen T, Häkkinen L, Hamidi S, et al. Laminin-5 expression is independent of the injury and the microenvironment during reepithelialization of wounds. *J Histochem Cytochem* 1998;46:353-360.

15. Michelson PH, Tigue M, Jones JCR. Human bronchial epithelial cells secrete laminin 5, express hemidesmosomal proteins, and assemble hemidesmosomes. *J Histochem Cytochem* 2000;48:535-544.

16. Nguyen BP, Ryan MC, Gil SG, Carter WG. Deposition of laminin 5 in epidermal wounds regulates integrin signaling and adhesion. *Curr Opin Cell Biol* 2000;12:554–62.

17. Sivaraman K, Chopra A, Narayan AI, Balakrishnan D. Is zirconia a viable alternative to titanium for oral implant? A critical review. *J Prosthodont Res* 2017;62:121–33.

18. Blanco J, Caneiro L, Liñares A, Batalla P, Muñoz F, Ramos I. Peri-implant soft tissue analyses comparing Ti and ZrO2abutments: an animal study on beagle dogs. *Clin Oral Implants Res* 2016;27:1221–6.

19. Rimondini L, Cerroni L, Carrassi A, Torricelli P. Bacterial colonization of zirconia ceramic surfaces: an in vitro and in vivo study. *Int J Oral Maxillofac Implants* 2002;17:793–8.

20. Scarano A, Piattelli M, Caputi S, Favero GA, Piattelli A. Bacterial adhesion on commercially pure titanium and zirconium oxide disks: an in vivo human study. *J Periodontol* 2004;75:292–6.

21. Shahramian K, Leminen H, Meretoja V, et al. Sol–gel derived bioactive coating on zirconia: Effect on flexural strength and cell proliferation. *J Biomed Mater Res - Part B Appl Biomater* 2017;105:2401–7.

22. Shahramian K, Abdulmajeed A, Kangasniemi I, Söderling E, Närhi T. TiO_2 coating and UV photofunctionalization enhance blood coagulation on zirconia surfaces. *Biomed Res Int* 2019;2019:8078230. doi: 10.1155/2019/8078230

23. Rossi S, Tirri T, Paldan H, Kuntsi-Vaattovaara H, Tulamo R, Närhi T. Peri-implant tissue response to TiO_2 surface modified implants. *Clin Oral Implants Res* 2008;19:348–55.

24. Areva S, Ääritalo V, Tuusa S, Jokinen M, Lindén M, Peltola T. Sol-Gel-derived TiO_2–SiO_2 implant coatings for direct tissue attachment. Part II: Evaluation of cell response. *J Mater Sci Mater Med* 2007;18:1633–42.

25. Areva S, Paldan H, Peltola T, Närhi T, Jokinen M, Lindén M. Use of sol-gel-derived titania coating for direct soft tissue attachment. *J Biomed Mater Res Part A* 2004;70A:169–78.

26. Paldan H, Areva S, Tirri T, et al. Soft tissue attachment on sol-gel-treated titanium implants in vivo. *J Mater Sci Mater Med* 2008;19:1283–90.

27. Lacoste-Ferré MH, Demont P, Dandurand J, Dantras E, Duran D, Lacabanne C. Dynamic mechanical properties of oral mucosa: Comparison with polymeric soft denture liners. *J Mech Behav Biomed Mater* 2011;4:269–74.

28. Hearn EJ. *Mechanics of Materials Volume 1 : An introduction to the mechanics of elastic and plastic deformation of solids and structural materials.* Oxford, UK:Elsevier;1997.

29. Willbold E, Witte F. Histology and research at the hard tissue–implant interface using Technovit 9100 New embedding technique. *Acta Biomater* 2010;6:4447–55.

30. Bako P, Bassiouni M, Eckhard A, et al. Methyl methacrylate embedding to study the morphology and immunohistochemistry of adult guinea pig and mouse cochleae. *J Neurosci Methods* 2015;254:86–93.

31. Sculean A, Gruber R, Bosshardt DD. Soft tissue wound healing around teeth and dental implants. *J Clin Periodontol* 2014;41:S6–22.

32. Tomasi C, Tessarolo F, Caola I, et al. Early healing of peri-implant mucosa in man. *J Clin Periodontol* 2016;43:816–24.

33. Berglundh T, Abrahamsson I, Welander M, Lang NP, Lindhe J. Morphogenesis of the peri-implant mucosa: an experimental study in dogs. *Clin Oral Implants Res* 2007;18:1–8.

34. Eming SA, Krieg T, Davidson JM. Inflammation in wound repair: molecular and cellular mechanisms. *J Invest Dermatol* 2007;127:514–25.

35. Salvi GE, Bosshardt DD, Lang NP, et al. Temporal sequence of hard and soft tissue healing around titanium dental implants. *Periodontol 2000* 2015;68:135–52.

36. Wong JW, Gallant-Behm C, Wiebe C, et al. Wound healing in oral mucosa results in reduced scar formation as compared with skin: Evidence from the red duroc pig model and humans. *Wound Repair Regen* 2009;17:717–29.

37. Abdulmajeed AA, Willberg J, Syrjänen S, Vallittu PK, Närhi TO. In vitro assessment of the soft tissue/implant interface using porcine gingival explants. *J Mater Sci Mater Med* 2015;26:1–7.

38. Moon IS, Berglundh T, Abrahamsson I, Linder E, Lindhe J. The barrier between the keratinized mucosa and the dental implant. An experimental study in the dog. *J Clin Periodontol* 1999;26:658–63.

39. Asoda S, Arita T, Takakuda K. Mechanical attachment of soft tissue to dental and maxillofacial implants with mesh structures: An experiment in percutaneous model. *J Biomed Mater Res - Part B Appl Biomater* 2013;101:553–9.

40. Steiniger BS, Bubel S, Böckler W, et al. Immunostaining of pulpal nerve fibre bundle/arteriole associations in ground serial sections of whole human teeth embedded in technovit® 9100. *Cells Tissues Organs* 2013;198:57–65.

41. Dhaliwal JS, Albuquerque RF, Murshed M, Feine JS. Osseointegration of standard and mini dental implants: a histomorphometric comparison. *Int J Implant Dent* 2017;3:15. doi:10.1186/s40729-017-0079-1.

42. Atsuta I, Ayukawa Y, Furuhashi A, et al. Epithelial sealing effectiveness against titanium or zirconia implants surface. *J Biomed Mater Res Part A* 2019;107A:1379-1385.

43. Burton HE, Freij JM, Espino DM. Dynamic viscoelasticity and surface properties of porcine left anterior descending coronary arteries. *Cardiovasc Eng Technol* 2017;8:41–56.

44. Craiem D, Armentano RL. A fractional derivative model to describe arterial viscoelasticitye. *Biorheology* 2007;44:251–63.

45. Gow BS, Taylor MG. Measurement of viscoelastic properties of the aorta in the living dog. *Criculation Res* 1968;23:111–22.

46. Saber-Sheikh K, Clarke RL, Braden M. Viscoelastic properties of some soft lining materials. I--Effect of temperature. *Biomaterials* 1999;20:817–22.

47. Peterson BW, He Y, Ren Y, et al. Viscoelasticity of biofilms and their recalcitrance to mechanical and chemical challenges. *FEMS Microbiol Rev* 2015;39:234–45.

48. Mesquita R V., Axmann D, Geis-Gerstorfer J. Dynamic visco-elastic properties of dental composite resins. *Dent Mater* 2006;22:258–67.

49. Suchatlampong C, Davies EH, von Fraunhofer JA. Some physical properties of four resilient lining materials. *J Dent* 1976;4:19–27.

50. Ho J, Tumkaya T, Aryal S, Coi H, Claridge-Chang A. Moving beyond P values: data analysis with estimation graphics. *Nat Methods* 2019;16(7):565-566.

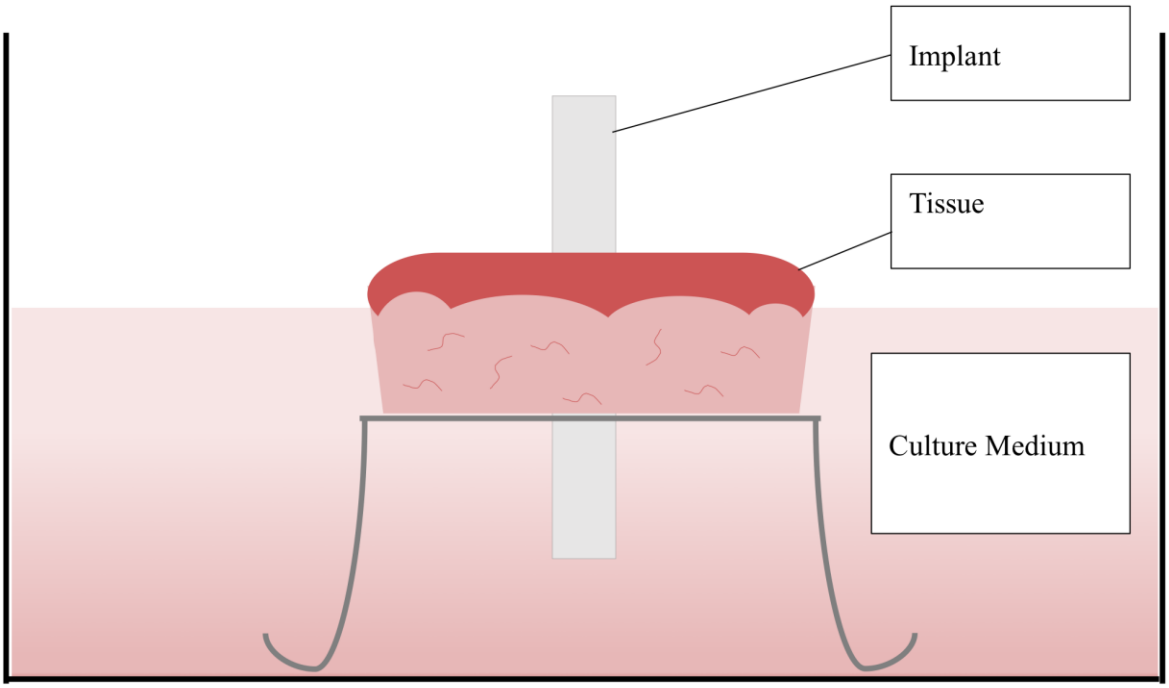

Figure 1. Schematic view of the culture model. Tissue/implant specimen is suspended in the culture medium at an air/liquid interface.

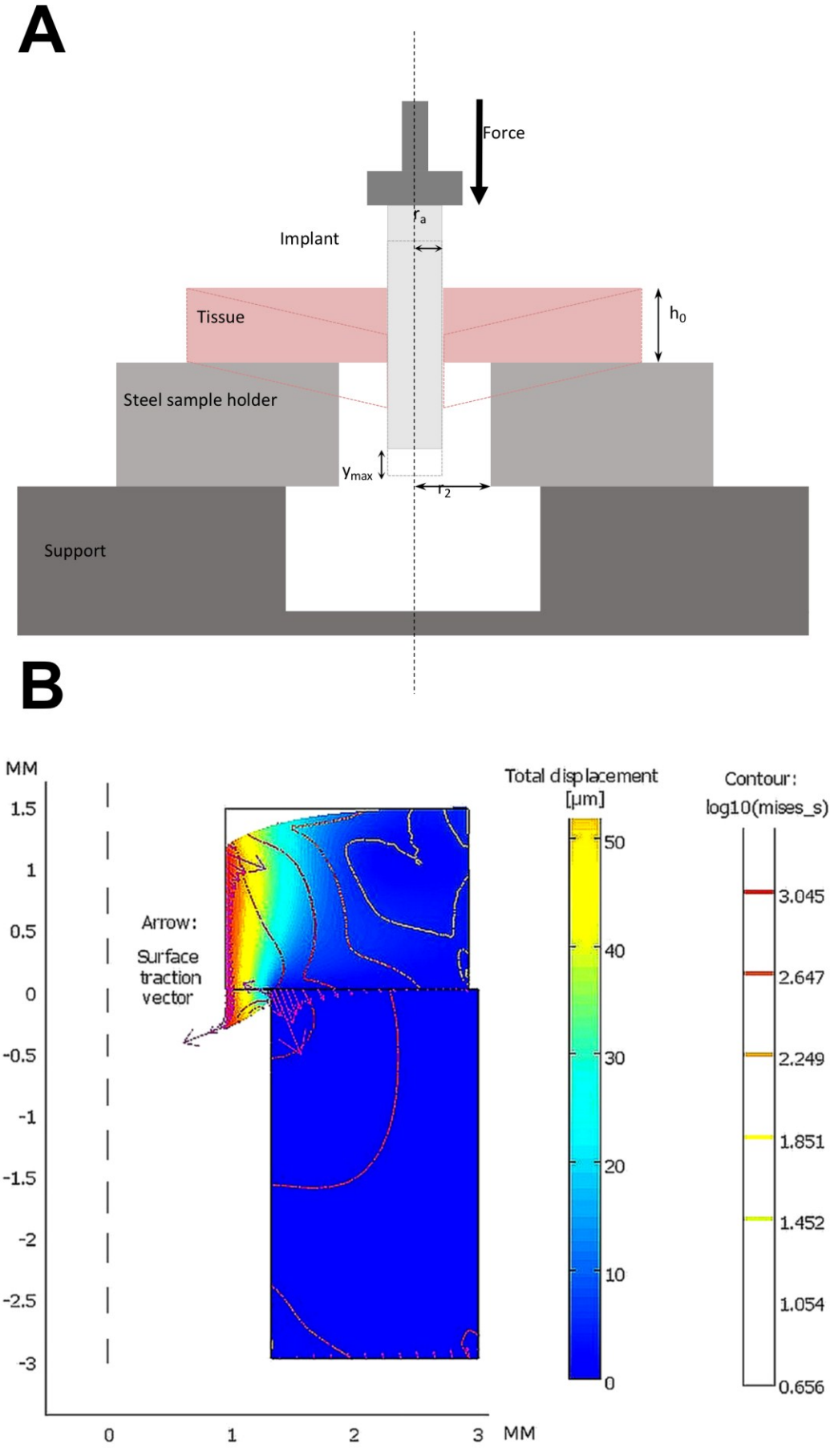

Figure 2. (A) Schematic view of the dynamic mechanical analysis test set-up and (B) computer model. Tissue holding implants are supported on a holder and dynamic loads are exerted on the top of the implant creating distortion in the tissue. The model (B) shows symmetric part of the tissue and the support with displacements, stresses and traction forces (see text for details).

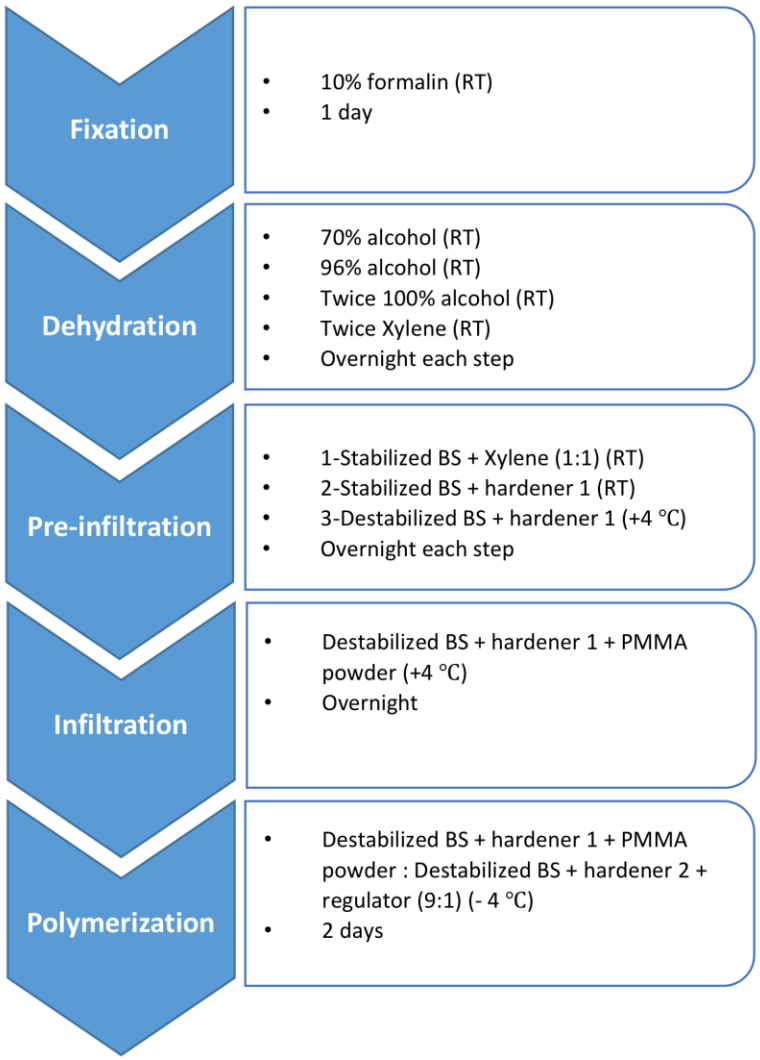

Figure 3. Steps, solutions and incubation times used in this study's modification of the novel embedding system . RT: Room temperature, BS: base solution.

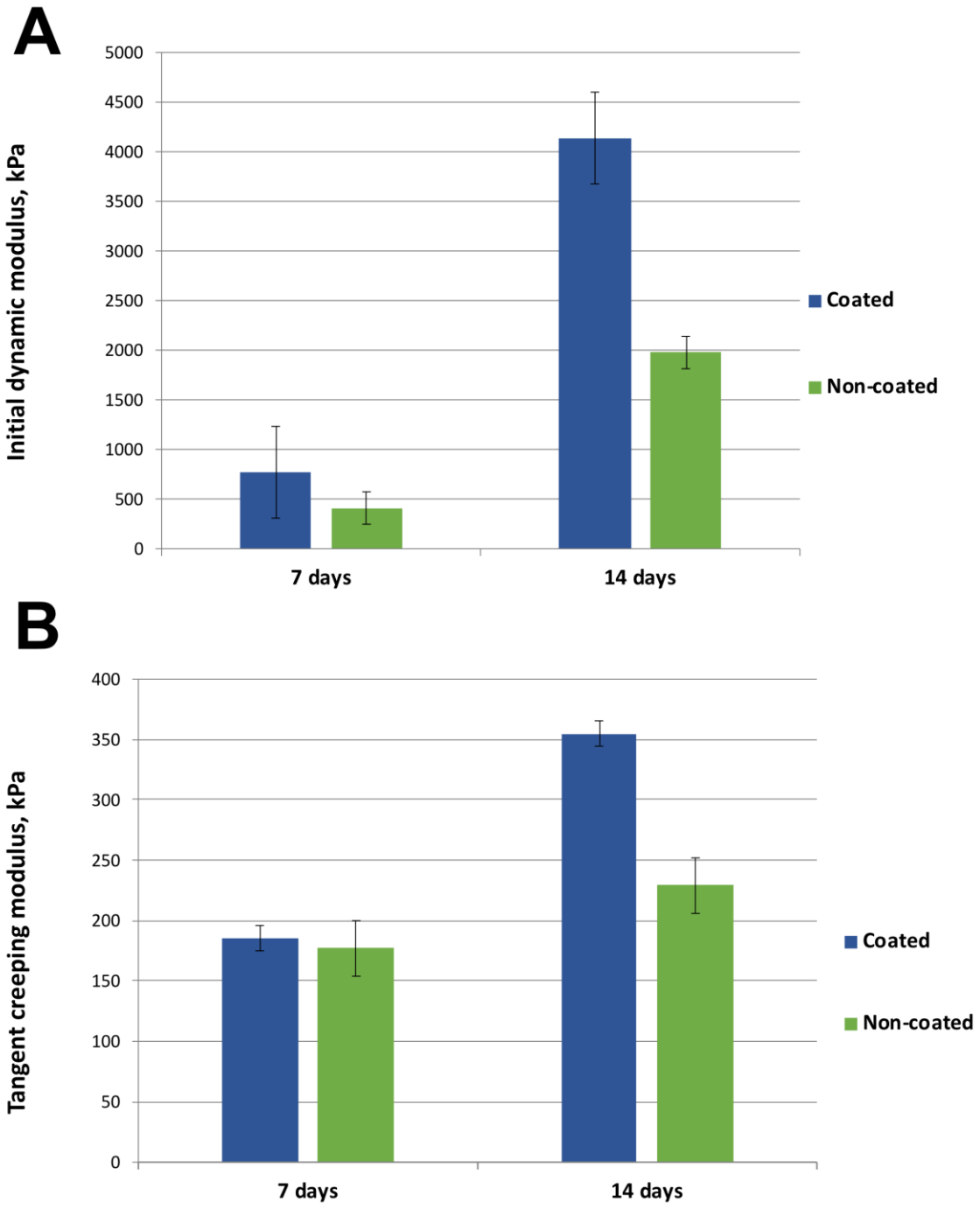

Figure 4. (A) Initial dynamic modulus of the tissue attachment apparatus calculated in both test groups at day 7 and 14 of culture (mean ± standard deviation). (B) Tangent creep modulus of the tissue attachment apparatus calculated in both test groups at day 7 and 14 of culture (mean ± standard deviation). For both groups n=2/time-point.

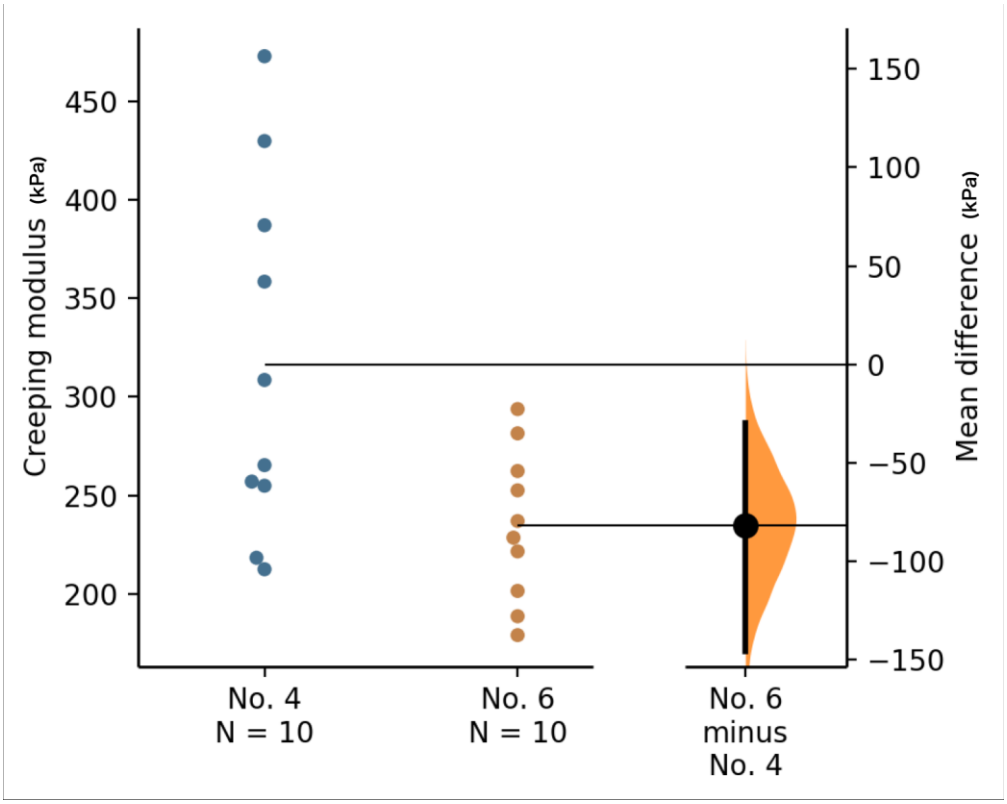

Figure 5. The mean difference between creeping modulus in dynamics (1 Hz) of one coated (No. 4) and uncoated (No. 6) samples are reported as Gardner-Altman estimation plot. Every measurement is taken at the same sample but at a different deformation amplitude (from 1 to 25 µm). Both groups are plotted on the left axis; the mean difference is plotted on a floating axis on the right as a bootstrap sampling distribution. The mean difference is depicted as a dot; the 95% confidence interval is indicated by the ends of the vertical error bar. The paired mean difference between No. 4 and No. 6 is -81.8 MPa [95.0%CI -146, -29.7]. The two-sided P value of the Mann-Whitney test is 0.0376. The effect sizes and CIs are reported above as: effect size [CI width - lower bound; upper bound] 5000 bootstrap samples were taken; the confidence interval is bias-corrected and accelerated. The P value reported is the likelihood of observing the effect size, if the null hypothesis of zero difference is true.

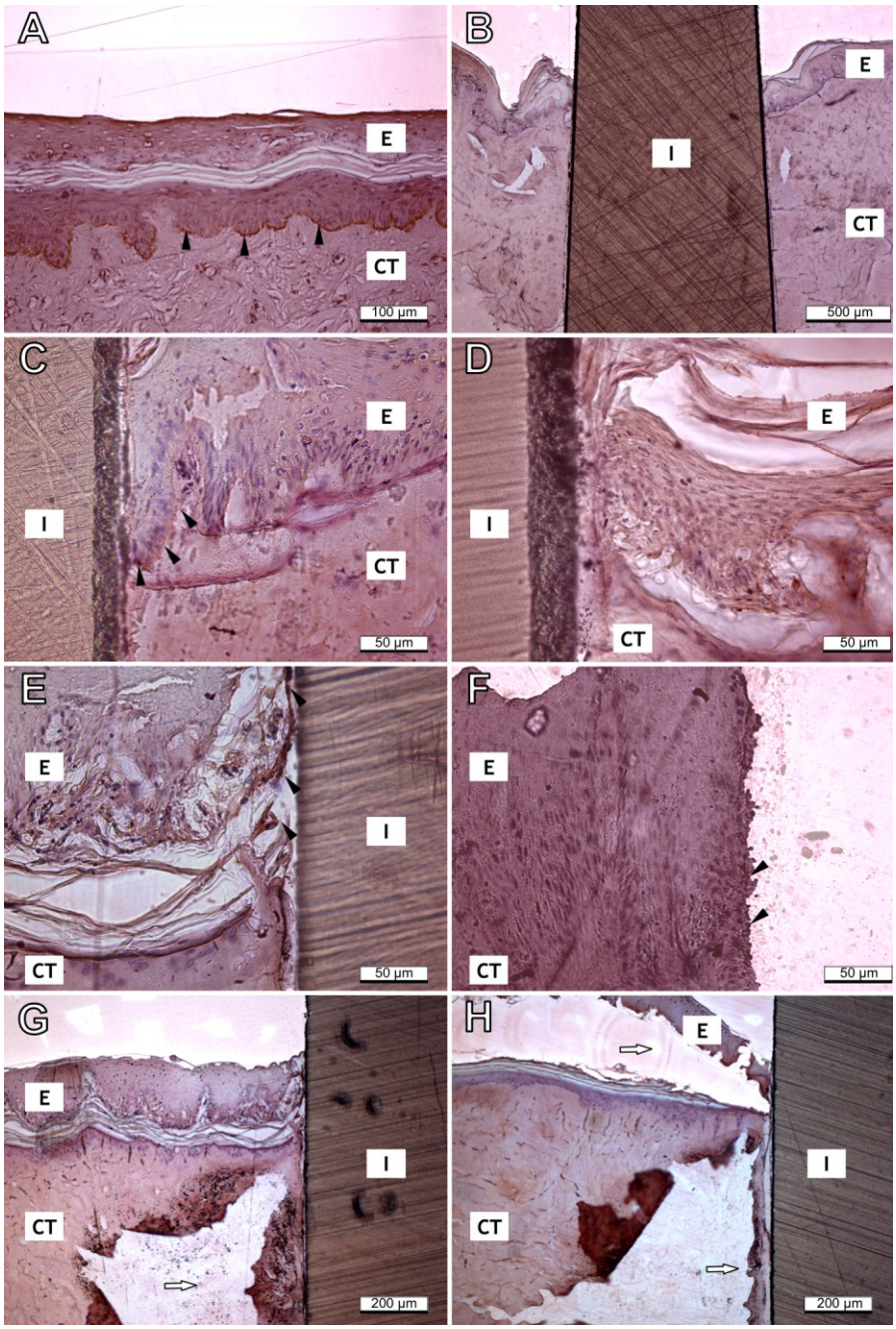

Figure 6. Light microscopy images of distribution of laminin γ2 in porcine gingival tissue and implant/tissue complexes cultured in vitro. E: epithelium, CT: connective tissue. I: implant. Hematoxylin counterstaining.

A. Porcine gingival tissue cultured at the air-liquid interface for 7 days and stained with laminin γ2 chain antibody specific for Ln-332. A clear staining can be detected at the basement membrane zone between the epithelium and the connective tissue (black arrow heads). The superficial layers of the gingival epithelium are sloughing off from the basal compartment of the epithelium, which is a phenomenon seen in all tissue cultures included the study.

B. A coated zirconia implant inserted in the middle of the tissue explant and cultured for 7 days in vitro. The epithelial and connective tissue are firmly attached to the implant surface.

C. A coated implant/tissue complex at day 7 of culture. A delicate laminin γ2 positive staining can be detected at the basal epithelial cells adjacent to the implant surface and at the basement membrane facing the gingival connective tissue (black arrow heads), but not in the cells attached to the implant surface.

D. A non-coated implant/tissue complex at day 7 of culture. Epithelial and connective tissue are attached to the implant surface, but laminin γ2 cannot be detected at the implant-epithelium interface.

E. A coated implant/tissue complex at day 14 of culture. Laminin γ2 is strongly expressed along the innermost layer of the epithelium with the coated implant surface (black arrow heads) despite the most coronal part of the epithelial attachment.

F. Porcine gingival tissue cultured for 14 days attached to the non-coated implant. The tissue has totally detached from the implant surface during cutting the tissue specimen (visual inspection) and the implant can not be seen in the figure. There are a few delicate spots of positive laminin γ2 staining detected at the surface of the epithelium that has been attached to the implant surface (black arrow heads).

G. A coated implant/tissue complex at day 14. The rupturing of the connective tissue (white arrow) in coated implant/tissue samples is seen 50-200μm away from the connective tissue-implant interface.

H. A coated implant/tissue complex at day 14 of culture. Despite sloughing of the uppermost epithelial cell layers (top white arrow), the upper part of the epithelium was still tightly attached to the body of the implant. Also, a thin layer of connective tissue is firmly attached to the implant (bottom white arrow).